JOURNAL OF MATERIALS SCIENCE 10 (1975) 870–888

Formation of bimodal crystal textures in polypropylene

P. G. ANDERSEN, S. H. CARR
Department of Materials Science, Northwestern University, Evanston, Illinois, USA

Electron microscopy, selected area electron diffraction, X-ray diffraction, and dynamic-mechanical testing have been used to study flow-crystallized and hot drawn isotactic polypropylene. As a result of these investigations, it was found that bimodal crystal textures can apparently be formed by at least two different treatments, but the corresponding morphologies are completely different. Flow-induced crystallization was observed to result in a microstructure of lamellae oriented perpendicular to the flow direction, while hot drawing of polypropylene films above a critical temperature produced a morphology of microfibrils lying parallel to the draw direction. Below this critical temperature, drawing produced a fibrillar morphology having only a typical unimodal fibre texture. As a result of information obtained here, a mechanism involving epitaxial deposition of chain segments onto growing lamellae is concluded to be responsible for formation of the bimodal crystal texture in flow-crystallized material.

1. Introduction

In addition to common spherulitic microstructures, two distinctly different morphologies can be created in semicrystalline polymer solids. One is produced by extensive plastic deformation and is characterized by microfibrillar crystallites oriented parallel to the draw direction. The other is produced by solidification from the melt in the presence of substantial flow and is characterized by lamellar crystallites oriented perpendicular to the flow direction. In either case the resulting chain orientation is parallel to the draw or flow direction. Creation of the microfibrillar structure has received considerable study [1-8] and resulted in several mechanistic models being proposed [2, 4-6] for its formation process. Robertson [4] recently hypothesized a model for the spherulite-to-fibril transformation based on the development and growth of kink bands, where the nature of the transformation implied that tie molecules between the original spherulitic lamellae comprise the microfibrillar backbone and that little unfolding of the crystalline chains occurs during this process. In another model proposed by Peterlin [2], the transformation from spherulitic structure into the parallel fibrillar structure occurs within a destruction zone defined by a plane of micronecks through which each lamellae passes and thereby becomes a system of parallel microfibrils. In contrast to Robertson's model, here some crystalline chains unfold in the destruction zone as shown by changes in small angle X-ray scattering properties. The long period of crystals in the new fibrillar structure has been found to be independent of fold period in the precursor lamellae but corresponds instead to the temperature of drawing [8]. Furthermore, Fung and Carr [1] have shown that deformation of flow-crystallized polyethylene fibres above their yield point results in tilting of lamellar crystallites that were originally oriented perpendicular to the flow direction. When a lamella had become sufficiently tilted toward the draw direction to the point that shear stress on $\{hk0\}$ planes exceeded some critical level, the crystal would transform into microfibrillar crystallites oriented parallel to the draw direction. Microstructures formed by crystallization from flowing melts have been studied to the point that some understanding has now been reached regarding their origin. Keller and Machin [9] and Hill and Keller [10] have proposed the existence of an extended microfibrillar crystal nucleus which forms in the melt parallel to, and as a result of, flow. These nuclei would serve as a central thread from which sets of lamellae can grow normal to them. This process is similar to that seen by Pennings *et al.*

[11] in crystallites solidified in a stirred solution, where the product resembles a "shish-kebab". Katayama *et al.* [12] studied crystallization of melt-spun fibres by taking X-ray diffraction patterns of the polymer at various points along the thread line. They found in all materials studied that the morphology consisted of lamellar platelets oriented perpendicular to the flow direction with their chains parallel to the flow. However, polypropylene was found to exhibit a second set of X-ray diffraction arcs corresponding to crystals in which their chain axes were perpendicular to the flow direction. This second population was noted to nucleate at some time following that of crystallites in the primary population; subsequently, both populations grew until complete solidification was achieved.

This bimodal, or two population, microstructure in isotactic polypropylene was first reported over a decade ago by Compostella *et al.* [13] and Awaya [14] who classified it as the "peculiar" structure of melt-spun polypropylene fibres. Later, Samuels [15] reported that cold drawn, compression moulded films exhibited only one population of crystallites whose *c*-axes were all parallel to the fibre axis but that upon annealing very close to T_m a second population of crystallites, whose *c*-axes were normal to the fibre axis were found to develop. Samuels proposed that these new crystals represented a high temperature structure in oriented isotactic polypropylene. Interestingly, Selikhova *et al.* [16], Khoury [17], Padden and Keith [18] and Binsbergen *et al.* [19] found a duplex growth habit of solution-grown single crystals of polypropylene, and each of the latter three suggested that this characteristic resulted from some form of epitaxial deposition of one crystal upon a preexisting lamella. They further suggested that this behaviour might exist in the bulk and be involved in creation of bimodal crystal textures in polypropylene solids. As an alternative explanation, Mencik and Fitchmun [20] presented evidence from recent work on injection moulding in which they interpreted a flow-crystallized morphology as being comprised of crystals with one orientation occupying a different zone from that occupied by crystals having the orthogonal orientation. Thus, there appears to be at least two alternative processes for preparing polypropylene solids having this bimodal crystal texture: (1) crystallization from flowing melts and (2) extensive deformation of solidified material at temperatures within a few degrees of the melting point. It is interesting to note that such a bimodal crystal texture, in which there is one population of crystals whose chains are oriented essentially normal to the elongation axis, seems at the present time to be exhibited only by polypropylene and not by the other, chemically similar macromolecular solids.

2. Experimental

Hexane-extracted Profax 6523 F (Hercules, Inc, Wilmington, Delaware) isotactic polypropylene was used in the preparation of the three sample types: (1) melt-spun fibres, (2) hot-pressed films and (3) flow-crystallized electron transparent films. Melt-spun fibres were produced as described previously by Fung *et al.* [21] by first extruding the polymer from an Instron Capillary Rheometer at a uniform rate, and allowing the molten filament to crystallize as it simultaneously cooled by natural convection and underwent extensions of about × 70. Various degrees of crystallite orientation were achieved by changing the draw ratio, but all fibres exhibited the characteristic flow-crystallized microstructure. Films of 0.005 cm thickness were prepared by hot-pressing moulding pellets of polypropylene at 215°C and then letting the film cool in the press; the resulting material had a spherulitic microstructure. After being removed from the press, the film was cut into 2.0 × 0.6 cm^2 strips, placed in the stretching apparatus, heated to various temperatures, T_D, and then stretched to different draw ratios, λ. Some films drawn at 125°C were subsequently annealed at 155°C for 1 h in either restrained or free (allowing retraction) conditions. Flow-crystallized electron transparent films were produced by evaporating a 0.02% solution of polypropylene in xylene onto a thin Mylar (E. I. duPont de Nemours Co, Inc, Wilmington, Delaware) film. The Mylar coated with polypropylene was placed in the stretching apparatus, heated to 180°C under flowing N_2 gas to melt the polypropylene, and allowed to cool quickly to 125°C at which point the Mylar substrate was stretched at a linear strain rate of 1 sec^{-1}. Because the polypropylene overlayer appears to adhere well to the Mylar, the polypropylene may be presumed to deform in the same manner as does its substrate, that is, by undergoing essentially uniaxial elongation. The solidified polypropylene overlayer was shadowed with a carbon–platinum mixture and then coated with a

water solution of polyacrylic acid. The polypropylene and dried polyacrylic acid were scored into squares and detached from the Mylar; then the polyacrylic acid was dissolved by placing the sample on a water surface. The remaining carbon–platinum shadowed polypropylene squares were then mounted on microscope grids for examination in a Hitachi 200F transmission electron microscope under bright field, dark field, and diffraction conditions.

Measurements of the complex modulus, E^*, its real and imaginary components, E' and E'', and the loss tangent, tan δ, were made on a Rheovibron dynamical-mechanical tester (Toyo Measuring Instrument Co Ltd, Tokyo, Japan). Film samples, 3 cm long, 0.2 cm wide and 0.00525 cm thick, were placed in the Rheovibron parallel to the draw direction and tested at 110 Hz in the temperature range − 100 to 130°C. Also, ten melt-spun fibres, 3 cm in length and 0.0058 cm diameter, were placed adjacent to each other to make a co-planar array which could also be examined in the Rheovibron.

Wide-angle X-ray diffraction photographs were taken of all the samples before and after being tested on the Rheovibron. The photographs were taken in a cylindrical camera using nickel-filtered Cu$K\alpha$ radiation at 40 kV from a Phillips X-ray unit. Also, X-ray photographs were taken of melt-spun fibres before and after being hot-drawn by various amounts.

3. Results

3.1. Bimodal crystal textures

Wide-angle X-ray diffraction photographs shown in Fig. 1 correspond to polypropylene prepared by the two methods: (1) crystallization induced by flow in the melt and (2) drawing of spherulitic films near their melting temperature. The equatorial arcs seen in the X-ray photographs are from a primary population of crystallites whose c-axes are parallel to the flow or the draw axis. Because all possible equatorial reflections are observed, it may further be inferred that a- and b-axes of these crystals are randomly oriented about the fibre axis. The meridianal arcs plus a contribution to the 040 equatorial scattering maximum result from a secondary population of crystals whose a-axes are nearly parallel to the fibre axis but whose b-axes are perpendicular to both the a-axis and incident X-ray beam. Although both methods will produce a bimodal crystal texture, there are slight differences in the resulting diffraction patterns. Spherulitic films drawn just below T_m, Fig. 1b, exhibit equatorial diffraction arcs which display the same amount of orientation as those of flow-crystallized (melt-spun) fibres. However, meridianal reflections for such drawn films are a single, broad arc. This contrasts with melt-spun fibres whose meridianal reflections consist of two distinct 110 maxima located 17° to either

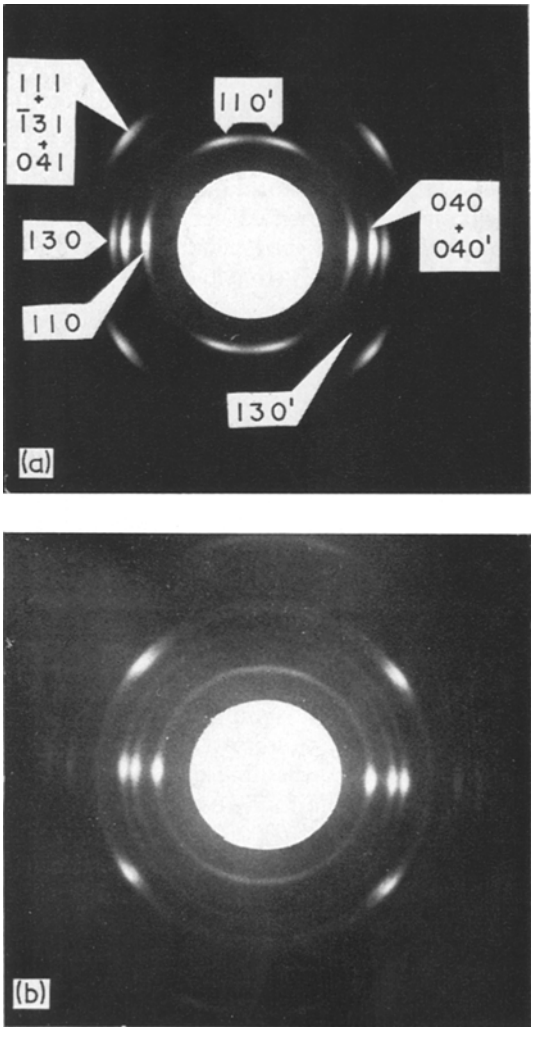

Figure 1 X-ray diffraction photographs from polypropylene samples containing a bimodal crystal texture. (a) From fibres whose well developed crystal texture was induced by flow in the melt; (b) from spherulitic films that were drawn near their melting temperature. Texture is not so well developed in hot-drawn films. Fibre axes are vertical. Primed indices designate reflections from second population crystals.

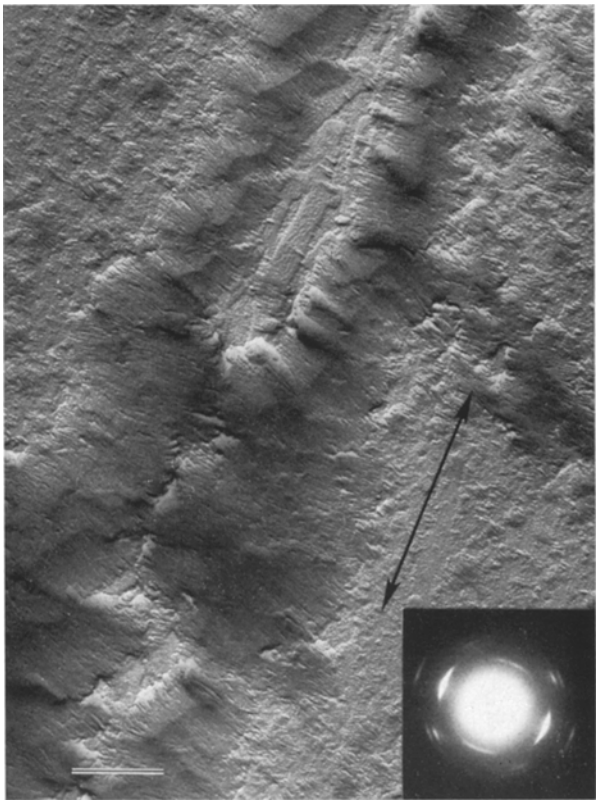

Figure 2 Electron micrograph of an electron beam-transparent polypropylene sample that had been flow-crystallized on a Mylar film while it was being stretched. The polypropylene exhibits a parallel structure of lamellar crystallites, oriented perpendicular to the flow direction (arrow). The bar indicates 1 μm.

side of the fibre direction. Thus, these two kinds of samples have equivalently well developed orientations of their primary population crystals, but with regard to their respective secondary crystal populations, the *a*-axis orientation is greater for melt-spun fibres than for hot drawn films. In addition to this difference in *a*-axis orientation, the relative intensities of reflections that appear on both meridian and equator (i.e. 110) are about equal for melt-spun fibres but are more intense on the equator than on the meridian for films drawn near their melting temperature. Presumably, this indicates a greater percentage of second population crystallites in melt-spun fibres than in the hot drawn films.

It has also been possible to duplicate these bimodal crystal textures in very thin, electron beam-transparent foils prepared under analogous conditions. Fig. 2 shows an electron micrograph of such a polypropylene sample that had been flow-crystallized on a Mylar film while it was being stretched. It can be seen in this micrograph that the polypropylene exhibits a parallel structure of lamellar crystallites which are viewed edge-on and oriented perpendicular to the flow direction (arrow). The diffraction insert reveals a normal complement of meridianal reflections, but reflections from only the (040) zone are seen along the equator, indicating some additional orienting influence must have acted upon the primary crystal population. Since the sample is a very thin foil, those lamellae seen in the micrograph probably nucleated directly on the Mylar substrate surface, and if there was a preference for the polypropylene to grow with its (100) planes parallel to the Mylar interface, then the observed orientation would have been expected. This specific orientation relationship between substrate and primary population crystals has, as a consequence, permitted a definite orientation relationship to be determined between primary and secondary crystal populations. Fig. 3

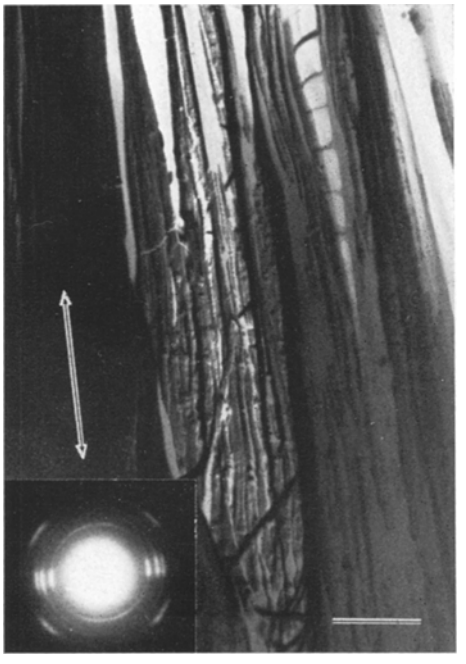

Figure 3 Electron micrograph of an electron beam-transparent polypropylene foil, initially having a random microstructure but which had been subsequently drawn near T_m. The crystal texture is similar to that of the flow-crystallized material, although the microstructure consists only of fibrils, oriented parallel to the draw direction (arrow). The bar indicates 1 μm.

displays an electron micrograph of polypropylene that had an initially random microstructure but had been subsequently drawn near T_m. Judging from its corresponding electron diffraction pattern, a very similar bimodal crystal texture also exists in this foil. However, the microstructure in this case is one of fibrillar units oriented parallel to the fibre axis rather than the lamellar structure possessed by the flow-crystallized foil seen in Fig. 2.

Using these X-ray and electron diffraction data, it is possible to define this orientation relationship between primary crystallites and those in the secondary population. As previously stated, both the *c*-axis of the primary population and the *a*-axis of the secondary population are parallel to the fibre axis. The electron diffraction insert of Fig. 2 shows that the only equatorial diffraction spots from the primary population are from the (040) zone. Since these arcs also include a contribution from the secondary population, it is therefore required that *b*-axes of both primary and secondary population crystallites be perpendicular to the fibre axis. The second population diffracts just as in the case of a bulk sample, where random *a*- and *b*-axis orientation of the primary population about the fibre axis is observed. This implies that in bulk samples the same crystallographic relationship exists between primary and secondary populations, as is defined by the diffraction pattern in Fig. 2. The relationship is shown diagrammatically in Fig. 4, where the *a*-axis of the primary population is parallel to the *c*-axis of the secondary population, the *c*-axis of the primary is parallel to the *a*-axis of the secondary, and the two *b*-axes are parallel.

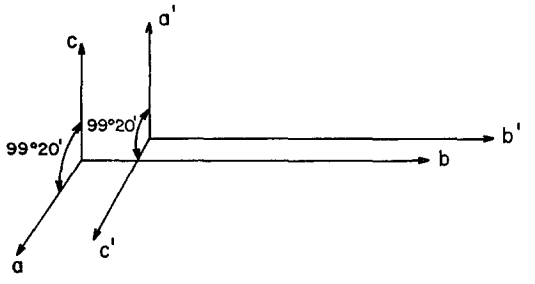

Figure 4 Schematic representation of the crystallographic relationship existing between the primary *c*-axis-oriented crystals and the secondary *a*-axis-oriented crystals. Primed symbols correspond to lattice vectors for second population crystals. For polypropylene, the specimen fibre axis would be vertical.

3.2. Plastic deformation

In an effort to achieve a better understanding of the microstructure associated with this bimodal crystal texture, specimens were subjected to plastic deformation by uniaxial tension. The four X-ray diffraction patterns displayed in Fig. 5 illustrate the effect of temperature, T_D, on high draw ratios, λ. Drawing at temperatures below 155°C produces a structure that gives a fibre pattern from a single population of crystals. However, drawing above 155°C produces a bimodal crystal texture that is rather similar to what was found in flow-crystallized material. However, the *c*-axis orientation was seen to be less well defined than in unimodal fibre patterns. Fig. 6 shows that increasing λ while drawing at 155°C simply increases the orientation of the bimodal structure. Finally, Fig. 7 illustrates the effects of annealing on films which had been uniaxially deformed at 125°C. It shows that

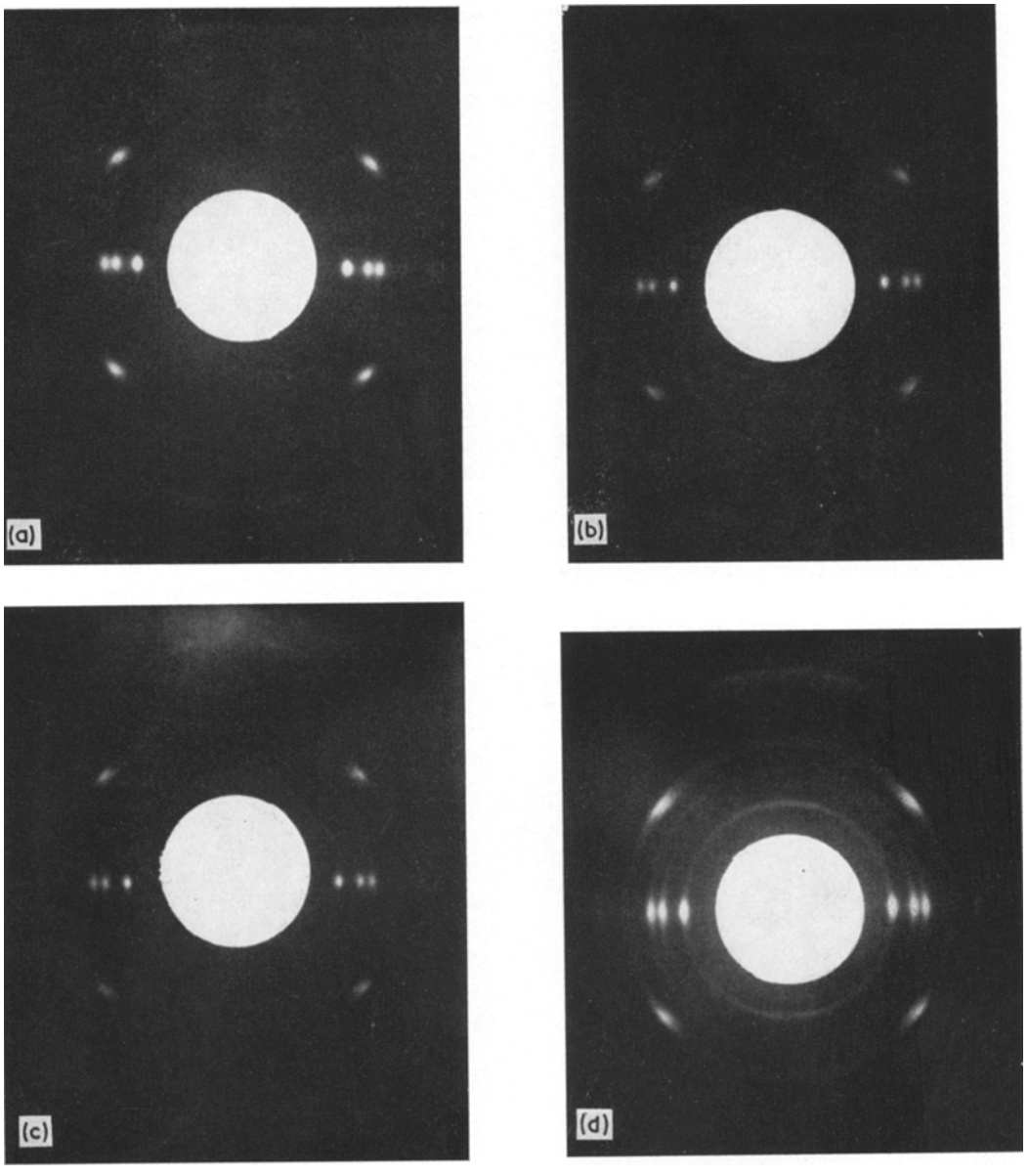

Figure 5 X-ray diffraction photographs of samples drawn to $\lambda = 9$ at (a) 125°C; (b) 150°C; (c) 153°C; (d) 155°C. The samples drawn below 155°C show a unimodal crystal texture, while that drawn at 155°C displays a bimodal texture. Fibre axes are vertical.

upon annealing within a few degrees of the melting point, an emergence of bimodality is not observed, as had been reported by Samuels [15] and Owen and Ward [22]. Although the annealing failed to produce a bimodal crystal texture, it did affect the orientation distribution of crystallites within this structure. Samples annealed unrestrained at 150°C show little orientation difference from the non-annealed sample. However, samples which remained restrained under tension showed a decrease in the arc of the diffraction spot and an increase in its 2θ half-width.

3.3. Dynamic-mechanical

The effect of hot-drawing and melt-spinning on the dynamic-mechanical properties of polypropylene was investigated to see what con-

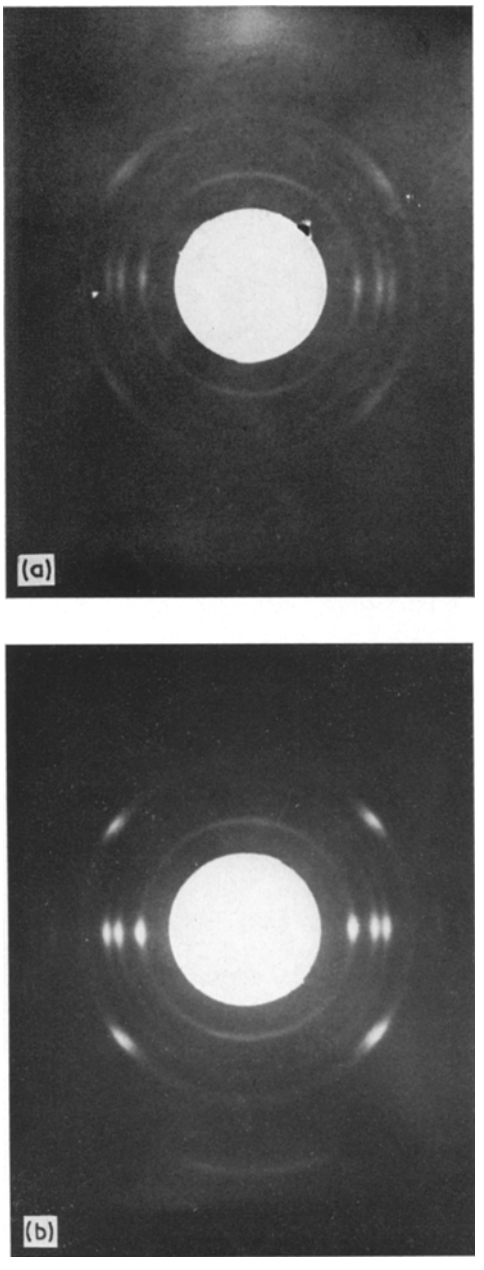

Figure 6 X-ray diffraction photographs of polypropylene drawn at 155°C. It can be seen that the orientation distribution of primary population crystals becomes more narrow as draw ratio is increased from $\lambda = 3$ (pattern *a*) to $\lambda = 9$ (pattern *b*). Fibre axes are vertical.

sequences the various crystal textures had on bulk specimens. Samples were divided in four groups. Group 1 permitted comparison of the difference between melt-spun fibres having a bimodal crystal texture, films drawn to $\lambda = 9$ at 155°C and, therefore, having a bimodal crystal texture, and a film having a spherulitic microstructure. Group 2 shows the effect of drawing spherulitic films to $\lambda = 9$ at various temperatures, while group 3 shows the effect of drawing to various draw ratios at 155°C, which develops the bimodal crystal texture. Lastly, group 4 samples were drawn at 125°C to $\lambda = 9$ and subjected to various annealing conditions at 155°C. Figs. 8a to d display real and imaginary components of complex tensile moduli as functions of temperature. Data useful in comparing these curves are contained in Table I, where $\Delta\tan\delta$ will serve as a quantitative measure of the magnitude of the β loss process. This peak is attributed to motions in chain segments within amorphous regions and was determined by subtracting tan δ at the peak maximum from an estimated background on a tan δ versus $1/T$ plot. Tan δ_{120} is the loss tangent at 120°C, and E'_{-50}, E'_{+50} are the real components of the tensile modulus at $-$ 50 and $+$ 50°C respectively.

Fig. 8a and the data for group 1 in Table I show that the flow-crystallized material, with its morphology of lamellar crystallites oriented perpendicular to the flow direction, has a lower elastic modulus than hot-drawn films in which there is an analogous bimodal crystal texture but a morphology of microfibrils oriented parallel to the draw direction. The explanation for this elastic modulus difference may lie in the relative magnitudes of movement that crystallites in these two microstructures can undergo because it has been shown (1) that applied tensile forces become resolved into bending and shearing couples, then it would follow that crystallites can bend in flexure and undergo interlamellar slippage. Even though it is reasonable to assume that the flexural moduli of crystallites in each kind of morphology are essentially the same, the larger lateral size of crystals in flow-crystallized polypropylene would lead to a larger amount of tensile strain than would be the case for crystallites in microfibrils at equivalent levels of flexure. Furthermore, the process [3-5] whereby lamellar crystallites become transformed by extensive uniaxial drawing (as presumably happens during formation of these hot-drawn films) would likely result in a higher surface density of tie molecules than would be created between lamellar crystallites nucleated in flowing melts. More tie

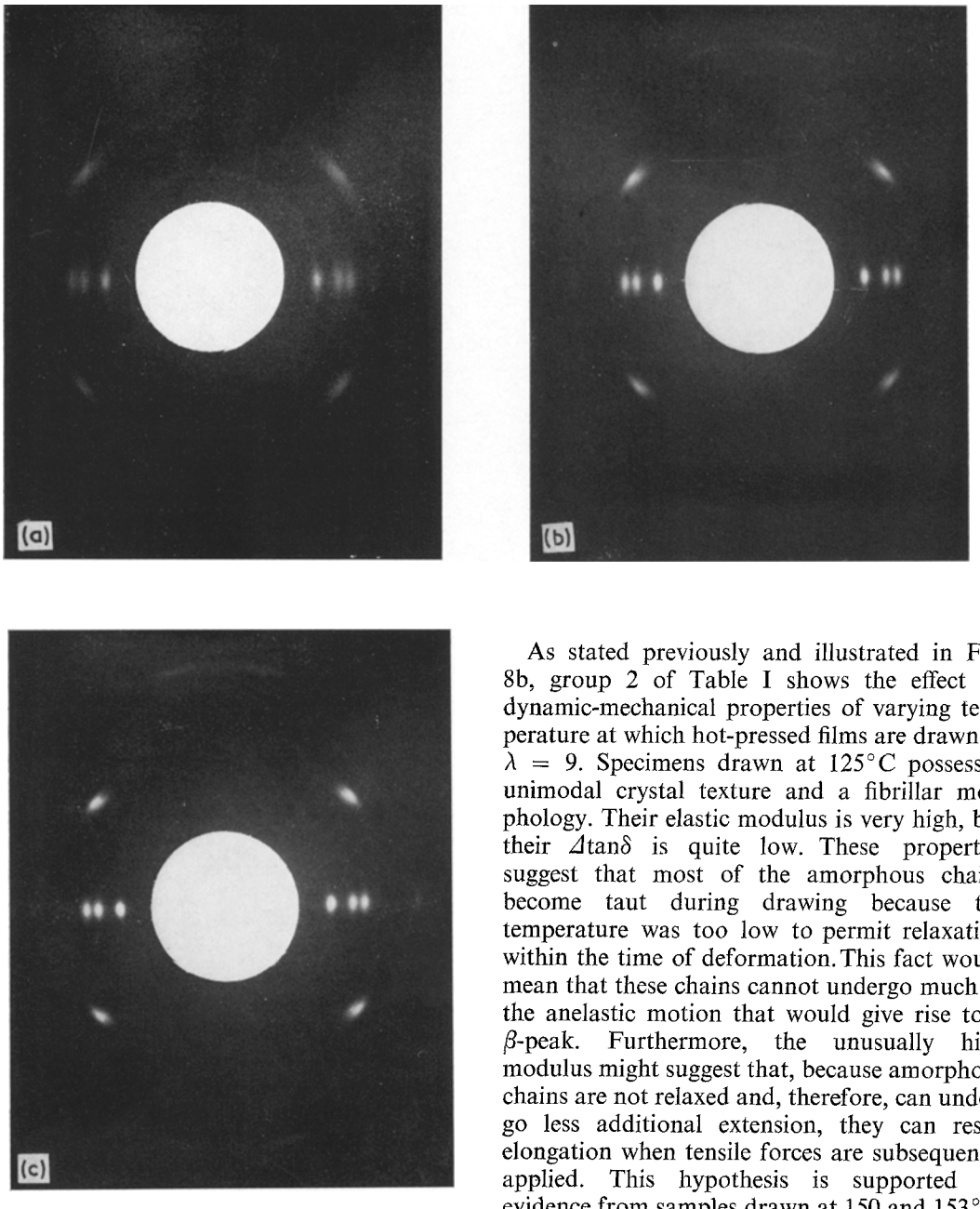

Figure 7 X-ray diffraction photographs of films which had been uniaxially deformed at 125°C. (a) $\lambda = 4$, no annealing; (b) $\lambda = 4$, unrestrained anneal shows little effect; (c) $\lambda = 4$, restrained anneal shows a decrease in the arc of the diffraction spot and an increase in the 2θ half-width. Fibre axes are vertical.

molecules would probably mean less interlamellar shear strain and so less accompanying uniaxial tensile strain.

As stated previously and illustrated in Fig. 8b, group 2 of Table I shows the effect on dynamic-mechanical properties of varying temperature at which hot-pressed films are drawn to $\lambda = 9$. Specimens drawn at 125°C possess a unimodal crystal texture and a fibrillar morphology. Their elastic modulus is very high, but their $\Delta\tan\delta$ is quite low. These properties suggest that most of the amorphous chains become taut during drawing because the temperature was too low to permit relaxation within the time of deformation. This fact would mean that these chains cannot undergo much of the anelastic motion that would give rise to a β-peak. Furthermore, the unusually high modulus might suggest that, because amorphous chains are not relaxed and, therefore, can undergo less additional extension, they can resist elongation when tensile forces are subsequently applied. This hypothesis is supported by evidence from samples drawn at 150 and 153°C, which have the same fibrillar morphology as samples drawn at 125°C but show slightly different dynamic-mechanical properties. It may be presumed that these variations reflect differences in their respective amorphous regions. For samples drawn at 150°C, it is probable that the temperature is high enough for amorphous material to relax during the drawing process and, therefore, the resulting solid would exhibit an increase in the relaxation peak. It is also noticed

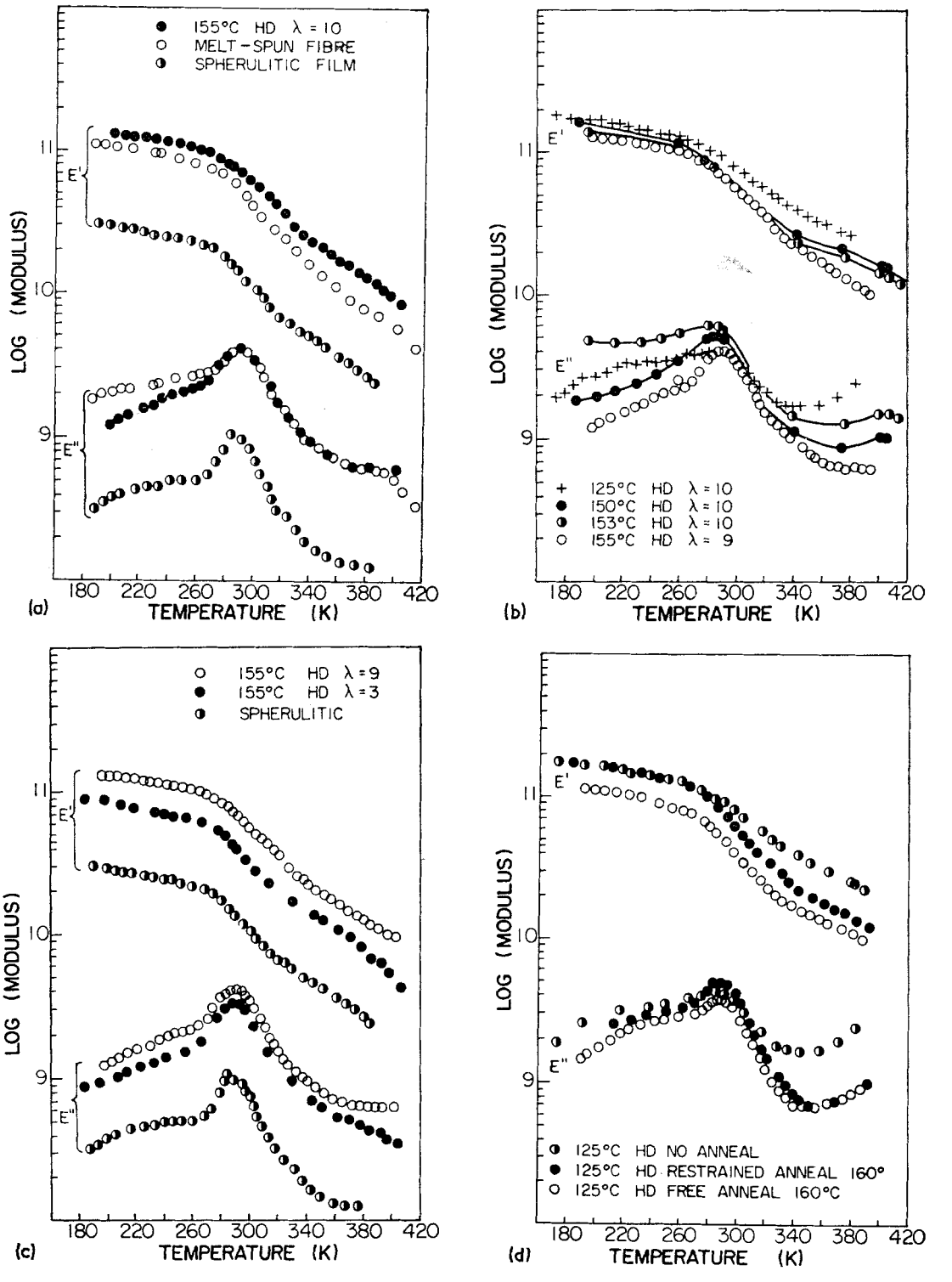

Figure 8 Real and imaginary components of the complex tensile modulus, E' and E'' respectively, shown as functions of temperature. Graph (a) shows that the flow-crystallized material with parallel lamellar morphology has a lower modulus than hot-drawn films with an analogous bimodal crystal texture, but a microfibrillar morphology. Graph (b) reveals that increasing the hot-drawing temperature of films causes them to have a lower tensile modulus. Graph (c) shows that increasing the draw ratio substantially increases the modulus. Graph (d) displays the effects of annealing on the tensile modulus of films drawn at 125°C. The modulus of the sample annealed under restrained conditions deviates from the modulus of the unannealed sample around the glass transition temperature, while the modulus of the freely annealed sample is always lower than either of the other two moduli.

TABLE I Summary of dynamic mechanical data for polypropylene

Group	Sample preparation	$\Delta \tan \delta$	E'_{-50} (10^{10} dyn cm^{-2})	E'_{+50} (10^{10} dyn cm^{-2})
1	Melt-spun fibre	0.0440	9.80	2.05
	Compression moulded film	0.0385	2.64	0.61
	155°C HD $\lambda = 9$*	0.0355	12.00	2.90
2	155°C HD $\lambda = 9$	0.0355	12.00	2.90
	153°C HD $\lambda = 10$	0.0460	14.00	3.20
	150°C HD $\lambda = 10$	0.0440	12.40	3.02
	125°C HD $\lambda = 10$	0.0155	15.00	4.88
3	155°C HD $\lambda = 3$	0.0555	7.00	1.65
	155°C HD $\lambda = 9$	0.0355	12.00	2.90
4	125°C HD $\lambda = 10$ no anneal	0.0155	15.00	4.88
	125°C HD $\lambda = 10$ free anneal	0.0425	9.95	2.00
	125°C HD $\lambda = 10$ restrained anneal	0.0450	15.50	3.00

*This designation stands for compression-moulded polypropylene films that had been hot-drawn (HD) at 155°C to a draw ratio, λ, of 9; designation of preparation for other samples is indicated analogously in this table.

that the β-peak for this drawing temperature is higher than the β-peak of the original spherulitic sample. This might suggest that in drawing the initially spherulitic samples, part of the crystalline structure is destroyed, thus increasing the amount of amorphous material in the drawn sample. Trends indicated in material drawn at 125 and 150°C appear to continue in specimens drawn at 153°C, where $\Delta\tan\delta$ increases and modulus decreases. However, drawing at 155°C affects the material differently than drawing at these lower temperatures. When the drawing is done at 155°C (very close to the melting temperature), it seems likely that there occurs some "premelting" of the kind reported by Iwato *et al.* [23]. As was described for drawing at lower temperatures, the amorphous chains must become pulled from their original configuration while the fibrils are forming, but they must also acquire an even greater ability to undergo relaxations to the point that some will recrystallize into second population crystallites. This would lead to a reduction in the amount of noncrystalline material and cause, therefore, a depressed value of $\Delta\tan\delta$.

Finally, Fig. 8d displays data for group 4, which shows the effect of annealing on dynamic-mechanical properties. Free annealing at 150°C lets extended and unrelaxed tie molecules undergo some retraction, as reflected by the 20% shrinkage of the specimen length. Although some of these chain segments might recrystallize, most must remain in the amorphous phase, thus accounting for the large β-peak and the decline in modulus. However, specimens annealed in the restrained condition cannot retract, and so relaxation of taut amorphous chains must be limited in the extent to which it can occur. The resulting new state of these amorphous chains would still possess some degree of extension and, consequently, the specimen modulus would be greater than in the case of freely annealed samples. Yet, enough relaxation of the amorphous chains must occur to cause its $\Delta\tan\delta$ to be greater than that of the freely annealed sample. In any case, the restrained annealing treatment does not appear to produce a solid whose properties approach those of films made by drawing at temperatures near the melting point.

4. Discussion

Work reported in the previous section has focused on two different preparations of polypropylene solids, one made by crystallization of flowing melts and the other made by drawing films at temperatures near the melting point. Each has an altogether different morphology, but both have very similar crystal textures. The bimodal orientation associated with each microstructure reflects the fact that during their formation process, a primary population of crystallites grew with their chains parallel to

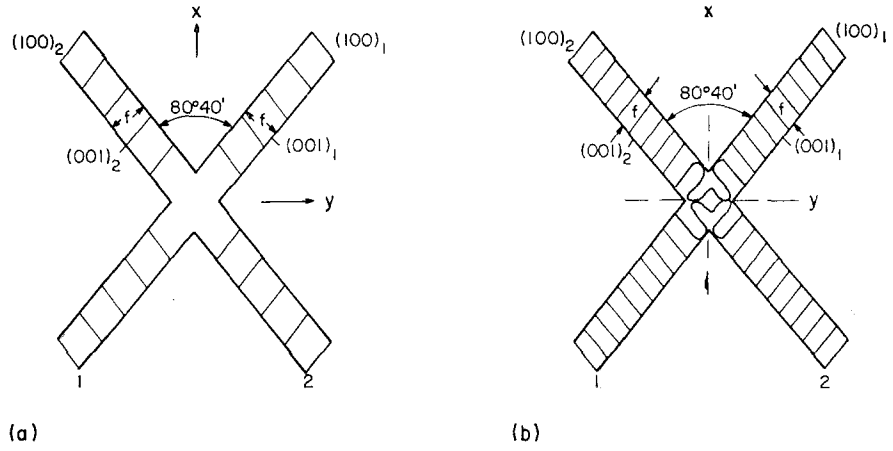

Figure 9 (a) Twinning model proposed by Khoury [17] to explain the growth of a dendritic crystal into an interwoven aggregate; (b) Twinning model showing in detail the unlikely nature, i.e. the required mirror image about the [101] direction, of such a truly twinned structure. Fold surfaces, f, are shown edge-on.

the draw direction, but subsequently a secondary population grew with chains oriented normal to those in primary crystallites. Formation of such a bimodal crystal texture under these preparation conditions seems, at the present time, to be a property exhibited uniquely by polypropylene, as crystallization of all other polymers under these conditions will produce a unimodal texture comprised only of crystals analogous to the primary population seen in polypropylene. Whatever the cause of this unusual crystallization behaviour, it must be derived from operation of a very specific mechanism, because these X-ray and electron diffraction studies have shown that the following orientation relationship (Fig. 4) exists between a primary and a secondary crystal: **a**′ is parallel to **c**, **c**′ is parallel to **a**, and **b**′ is parallel to **b** (primes designate those lattice vectors for the second population).

It is interesting to note that such a coupled, bimodal crystallographic orientation has also been reported previously to exist [16-19] in polypropylene crystallized in the absence of flow or hot-drawing conditions. Using X-ray microcamera techniques and birefringence studies on large crystalline aggregates grown by slowly cooling concentrated polypropylene solutions, Selikhova *et al.* [16] concluded that they had produced a kind of biaxial crystal. Similarly, Koury [17] proposed two alternative models to describe the interwoven structure of such solution-grown crystal aggregates. From these models it was suggested that growth of a dendritic crystal into an interwoven aggregate involved repeated twinning of the crystal about an axis at right angles to the **b** crystallographic axis and almost coincident with [10$\bar{1}$], as shown in Fig. 9a. However, it is quite unlikely that this is a true twin, since a complete mirror image about the [10$\bar{1}$] direction, as shown in Fig. 9b, would have to exist. Unfortunately, such a structure is a very unlikely possibility. A more probable mechanism by which two crystals can grow into aggregates of orthogonal elements would be by epitaxial deposition and growth of secondary crystals onto an original one. However, this idea also presents some problems since it might require that the secondary nucleus would have to be deposited onto a fold surface. Although it is possible that primary crystals have a perfectly regular fold surface, this is likely not to be the case. Therefore, the epitaxy mechanism, if applicable, must operate with assistance of as yet unidentified effects.

Padden and Keith [24] investigated branching in aggregates of interwoven polypropylene similar to Koury's and concluded that (010) lateral surfaces are the initial sites of branching and that this branching results from some form of epitaxial attachment. This would require the *c*-axis of a branch to attach epitaxially parallel to the *a*-axis of the parent crystal, but this process would be accompanied by 2% lattice mismatch. However, it has been proposed more recently [18] that such epitaxial nucleation, which can

lead to branches of second population crystallites, starts with an overgrowth having the γ crystallographic phase. In this case, the mismatch between a-axis of the parent and the c-axis of the γ phase is only 0.6%. This is consistent with their observation that the γ phase exists only when the system is allowed to crystallize slowly between 138 and 142°C. Work by Kardos *et al.* [25] which shows that the γ phase transforms to the more stable α phase when cooled below $\sim$ 147°C supports this concept. However, in our work it has previously been shown that drawing at 155°C, which is above the stable temperature for the γ phase, still produces a bimodal crystal texture. Thus, it seems that epitaxial deposition may be involved in the mechanisms whereby a second population nucleates on existing crystals with this special orthogonal relationship between them, but other factors must also play a role in this process, as well.

Although epitaxial deposition onto a folded chain surface seems unlikely for the polypropylene aggregates discussed previously, it might be more probable for the case of flow-crystallized systems. Keller and Machin [9] and Hill and Keller [10] and Garber and Clark [26] have proposed the existence of central threads as being the backbone of the parallel stacks of lamellae. Although there may be some reason [1] to question whether there is any appreciable concentration of central threads in these solids, it has already been shown [27] that crystallization from stirred supersaturated solutions does not necessarily involve epitaxial crystallization of platelets on central thread structures. Whatever the case may be, it can be supposed that local flow (especially if it is extensional in character [28, 29]) will impart a preferred chain orientation which would reduce the entropy of this system and, therefore, the work needed to nucleate a solid from it. Orientation of chain segments would also impart a unidirectional alignment to the crystallites in the resulting morphology. Then the picture becomes one in which the initial embryonic crystal nucleus is either an extended-chain fibrillar unit or an object unit in which partly folded chains lie parallel to the flow direction. Crystallization can only proceed laterally because of limitations imposed by chain-folding. The resulting tie molecule density between growing lamellae would then depend on the number of initial crystallites to which a chain extended by the local flow field had access. Direct observation of the flow-crystallized morphology (Fig. 2) reveals stacks of parallel lamellae that are approximately 250 Å thick. Although there may be resolvable gaps between lamellae in the final structure, it cannot be said whether an appreciable spacing had existed between them while the system was freezing. For example, if such gaps were present but of sufficiently small dimension that a critical nucleus could only form with its chains in the plane of the gap, then it would follow that these crystallites would exhibit chain orientations normal to the flow direction. Furthermore, if this were the only constraint affecting their orientation, then their a- and b-axes would grow in random directions. However, this is not found to be the case with second population crystals in bimodal polypropylene, as only a-axis orientation in the fibre direction is observed. This additional degree of orientation may be due to the way in which chains in these narrow gaps can add to such a growing crystallite. It is envisioned that chains (or segments of tie molecules) occupying this interlamellar gap are strained to some degree due to stress on the entire collection of crystals, and as a result, it will be most favourable for them to fold onto crystal growth faces that are parallel to their strain (fibre axis) direction. Because the fold planes in polypropylene lamellae are understood [30] to be {0 1 0}, then it would follow that addition of such partly strained chain segments to build successive monolayers of folded chain segments in these growing crystallites would result in b-axes growing in the plane of the gap. Consequently, the a-axes would become oriented normal to the plane of the gaps (and parallel to the fibre axis). Therefore, one possible model is shown in Fig. 10, where the second population is sandwiched between lamellae but has the properly observed crystallographic relationships.

Another model, in which the second population is part of, or adjacent to, the lamellae and results from truly epitaxial deposition, is shown in Fig. 11. As the lamellae grow laterally, a free chain could attach itself onto the growing b face in such a way that it would grow with a second population orientation. Subsequent layers of chain segments could either be placed as part of the second population crystallite or their orientation could revert to that of the primary orientation. Eventually, this crystallite would be sandwiched between two lateral sections of primary crystal-

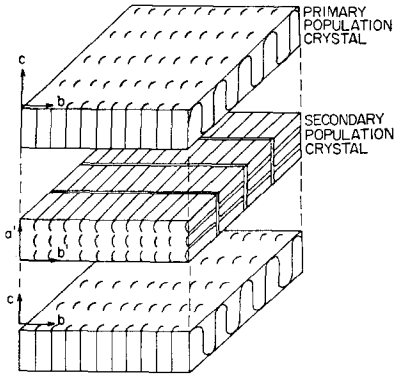

Figure 10 A possible model for the bimodal crystal texture of polypropylene where the second population crystallites, with the proper orientation, are sandwiched between lamellae of primary crystallites.

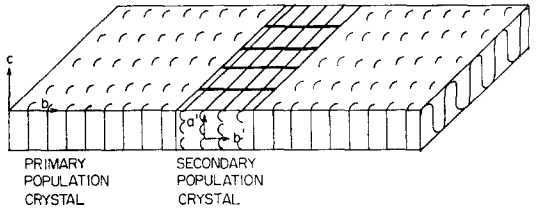

Figure 11 An epitaxial model for the bimodal crystal texture of polypropylene where the second population crystallites are part of, or adjacent to, the primary population lamellar crystallites.

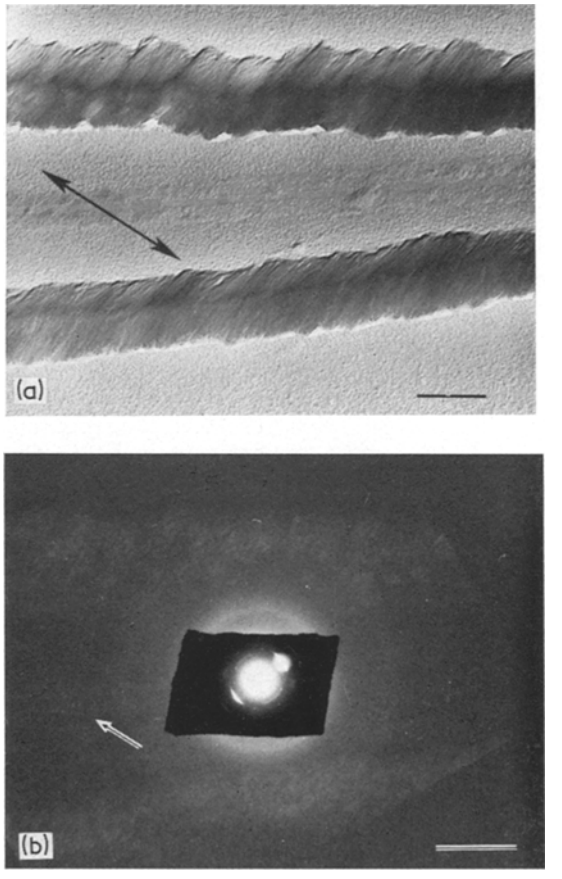

Figure 12 (a) Bright-field (b) dark-field electron micrographs of an electron beam-transparent polypropylene film solidified during elongational flow (parallel to arrow in a). The corresponding diffraction pattern was recorded by a double exposure technique (and has had its intensity adjusted to the dark-field image by dodging); the highlighted reflection was used to produce the dark-field micrograph. The dark-field micrograph (b) reveals a gap (in the region indicated by the arrow) between the primary population lamellae, as would support the sandwich model, but also shows a discontinuity along the lateral direction of the lamellae, which would support the epitaxial model. The bars indicate 1 μm.

lites or be the end of the lamellae. The micrograph in Fig. 2, if carefully examined, provides possible evidence for this sequence of events; there seem to be depressions along some of the lamellar edges which may actually be due to parts of second population crystals. Also, the dark-field micrograph in Fig. 12 shows discontinuities along the lateral direction of the lamellae (as indicated by the arrow). Furthermore, epitaxial deposition of polypropylene without the γ phase would seem possible, since the 2.3% lattice mismatch between the *a*- and *c*-axes of the two crystal populations is actually quite small. Consistent with this model, Binsbergen *et al.* [19] note that lattice matching is a necessary but not sufficient condition for epitaxial deposition to be controlling in crystallization of polypropylene. They showed that methyl groups of one plane fit rather well into depressions in its neighbour, but when a layer is rotated, as might correspond to the relationship between primary and secondary crystals, this same match between methyl group and depressions remains.

An additional set of experiments were performed in an effort to differentiate between these two models. A melt-spun fibre that produced the diffraction pattern shown in Fig. 13b was heated to 150°C and stretched 70%. It can then be noticed that the pair of 110 second population maxima (arrows) have undergone rotation by 70° in both clockwise and counterclockwise directions, while the equatorial reflections have

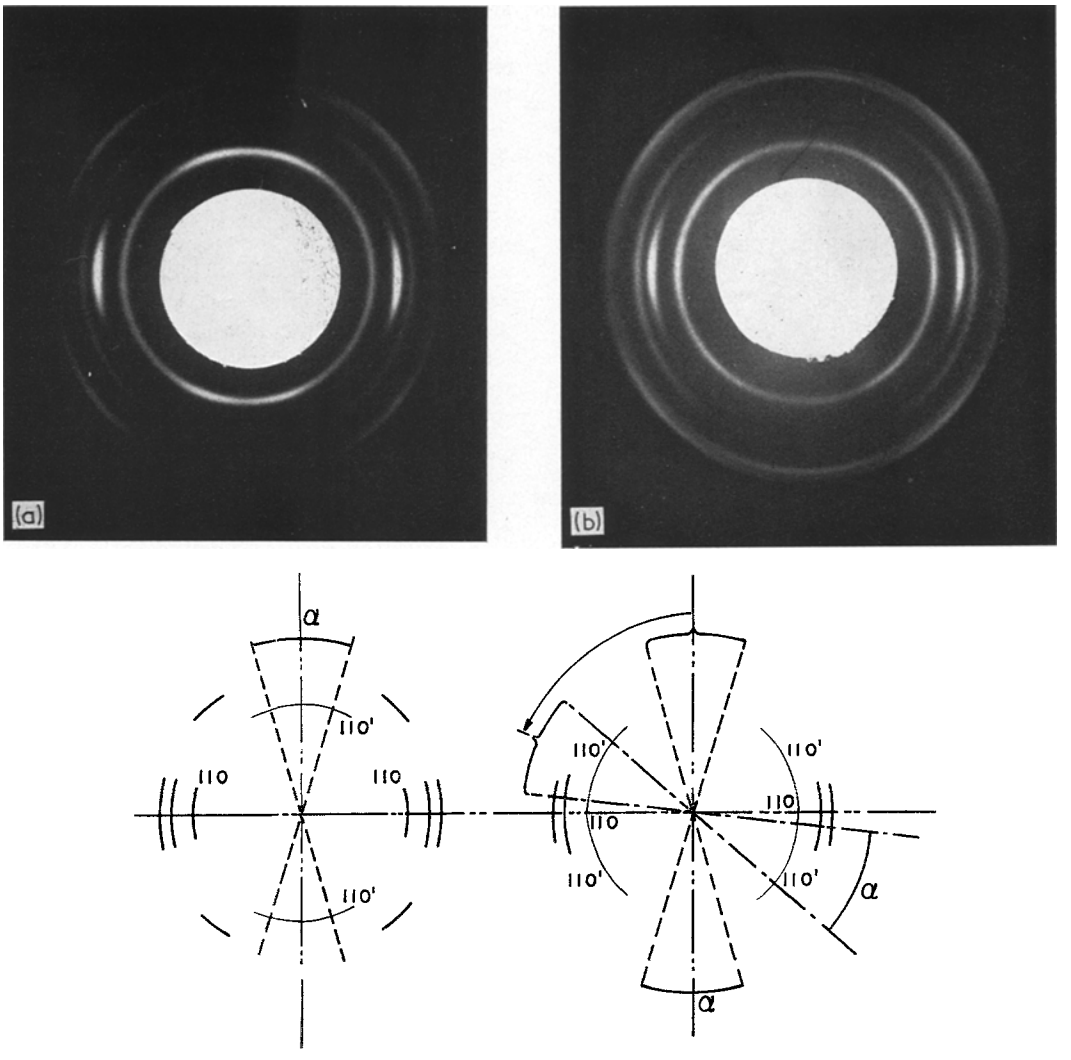

Figure 13 Photographs and schematic representations of X-ray diffraction patterns from the melt-spun fibre before (a) and after (b) being heated to 150°C and stretched 70%. The schematic pattern in (b) shows the anticlockwise rotation (arrow) of meridianal second population 110 reflections due to stretching; an analogous clockwise rotation of reflections is also seen to occur as a result of this deformation. α indicates the characteristic angular length of these 110 reflection arcs and is seen to remain essentially constant during deformation. Primed indices designate scattering from the second population crystals. Fibre axes are vertical.

remained essentially unchanged in terms of location (but increased in the intensity of 110 maxima due to coincidence of reflection from both primary and secondary crystals). There are several possible explanations for this behaviour; however, none are completely satisfactory. The first explanation is illustrated in Fig. 14. Here a primary crystallite is rotated about its a^*-axis, as it would do as the solid undergoes this deformation. However, intralamellar slippage allows chains to remain parallel to the draw direction, as deduced from the constancy of the equatorial spots. On the other hand, it can be seen that second population crystallites become rotated without any similar chain slippage. These motions require that slippage between the primary and secondary crystallites must occur, so this is either a case in which these two kinds of crystals are not attached to each other or one in which chains are pulled from crystals during

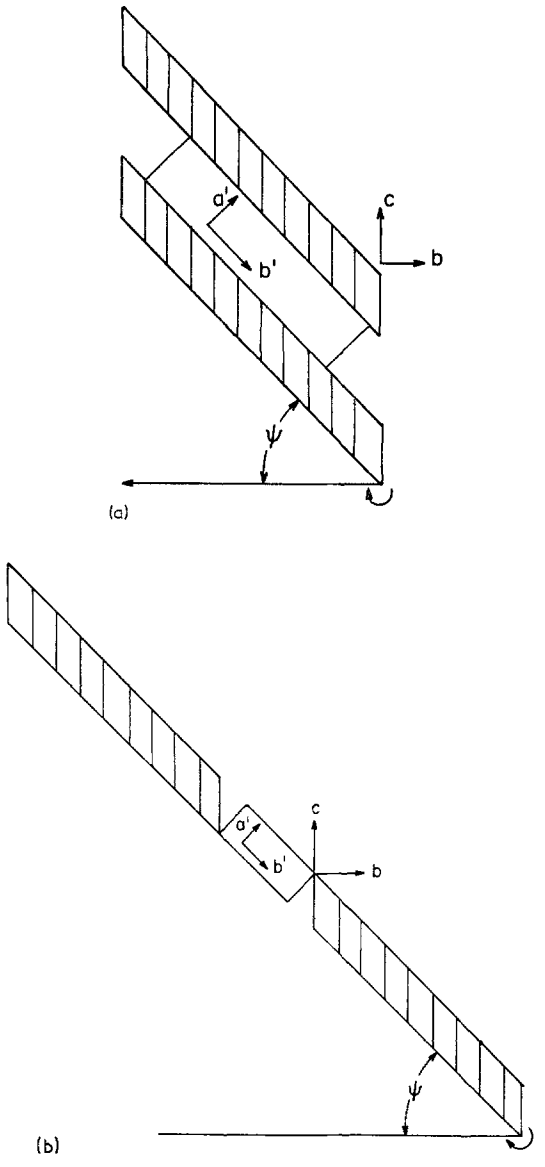

Figure 14 Illustrations of the rotation of a crystallite about the *a*-axis. Both models show that the orientation of chains in the primary population remain constant, while the second population rotates without similar chain reorganization. Model (a) requires slippage between the primary and secondary crystallite while (b) requires the two crystallites must separate at the point of epitaxial contact.

deformation. This latter effect seems more likely because below a critical temperature for a 70% deformation, no permanent rotation of the 110 meridinal spots can be observed. In Fig. 14b the rotation of the epitaxial model about the *a**-axis is shown, but to achieve this rotation, the two crystallites must separate at the point of epitaxial contact. However, analogous rotations in reflections for (040) and (130) planes, which might also be predicted by such rotations of secondary crystallites, are not readily seen. This may be due to their larger diffraction angles which result in their being rotated more readily out of diffraction condition.

Although this discussion has centred around flow-crystallized material in general, it applies also to bimodal hot-drawn films. In plastic deformation of spherulitic polypropylene, the non-crystalline chains gain increased levels of mobility as the draw temperature increases toward T_m. This is supported by results which show increased $\Delta\tan\delta$ peaks corresponding to increased drawing temperatures. The rise in $\Delta\tan\delta$ was hypothesized to result from greater chain mobility which allowed them to undergo increased relaxation while being drawn. However, when the draw temperature is sufficiently high that the bimodal crystal texture forms, a slightly lower $\Delta\tan\delta$ value is observed. Thus, it can be reasoned that chains in the destruction zone, which is sufficiently disordered that it approximates a melt, approach the same state as those in a flowing melt. Then, as the film is drawn, some of the chains that ordinarily would not crystallize can undergo appropriate ordering.

5. Conclusions

The question still remains regarding which is the more probable of the two models for the formation of bimodal crystal textures: geometrical constraints placed upon crystallizable interlamellar material, or epitaxial attachment of chains to a growing lamellar crystallite. From the information presented, support of the interlamellar crystallization process based on entrapped chains and loose chain ends has at least one major difficulty. This arises from the fact that the fast growth direction of polypropylene crystals is actually parallel to the *a*-axis. The consequence of this fact is that crystals growing in interlamellar regions and having chains lying in the plane of interlamellar spaces would tend to propagate with their *a*-axes perpendicular to the flow direction. This would result in a *b*-axis orientation for such second population crystals that is normal to *b*-axes of primary crystallites, while, in fact, a parallel relationship was determined experimentally to be the case. Only if there would be a high surface density of nucleation

sites within such interlamellar zones would it be possible to get enough crystals with both *c*-axes and *b*-axes perpendicular to the flow direction to satisfy the X-ray observation of nearly equal amounts of primary and secondary crystals. On the other hand, the epitaxial deposition process does not limit growth of second population crystals by the above constraints. Further, this proposition offers the additional attraction of predicting the specific crystallographic orientation relationship which is always observed between these two crystallite populations. Therefore, it is concluded by this work that of the two processes, the one involving epitaxial secondary nucleation seems more applicable to explaining the origin of bimodal crystal textures in oriented polypropylene. However, because no direct test of this conclusion has been performed, it is possible that neither of these hypotheses is correct; rather, some other, as yet unidentified, combination of crystallization processes may actually be operative to create this special bimodal crystal texture in polypropylene.

A probable growth model for flow-crystallized polypropylene based on the epitaxial deposition of chains can be developed from this information. First, nucleation and initial growth of primary population lamellae oriented perpendicular to the flow direction [12] occurs as a result of the chains being oriented parallel to the flow direction. Extended chain tie molecules between vertically adjacent lamellae would be the load bearing linkages and, consequently, the major flow stresses would be transmitted through the system by stacks of parallel lamellar crystallites. It would follow that there would exist at the perimeter of the laterally growing lamellae a zone of relatively relaxed melt in which chains would not be subject to strong orientation effects. It would be this lack of orientation parallel to the flow direction which might then permit epitaxial nucleation and growth of second population crystallites to occur. As crystallization would continue, the growth of a second population crystallite could revert back to growth with primary orientation or it could be impinged upon, and combine with, another growing nucleus to form one larger lamellae from two smaller ones. Therefore, this growth mechanism would result in the final lamellae consisting of interspersed primary and secondary population crystallites. This growth model then is consistent with results of Katayma *et al.* [12] which show the simultaneous growth of primary and secondary crystallite populations at later stages of freezing.

In view of this proposed mechanism, a possible explanation can be offered for differences between the percentage of second population crystallites in the flow-crystallized structure (approximately 50%) and the hot-drawn material (approximately 10%). Crystallization from a flowing melt involves a situation in which regions near certain crystal faces are occupied by relatively relaxed chains, and as a result, there is ample opportunity for secondary nucleation events to start crystals with the second population orientation. However, during the plastic deformation of spherulitic polypropylene, at elevated temperatures, it is envisioned that there is some disorder acquired by the material, but it is confined within a very small zone through which each portion of a lamellar crystal passes as it converts into a microfibrillar unit. Thus, the percentage of chains having mobility equal to that of chains in the melt is very greatly decreased, and correspondingly, the number of chains available for formation of a second population crystallite is decreased.

From the mechanism proposed above, and taking into account the dynamic–mechanical data, it may be inferred that the production of hot-drawn polypropylene with a bimodal crystal texture would be accompanied by an increase in the density of tie molecules between crystallites. This increased density would likely hinder any growth of second population crystallites between primary crystallites, leaving only the lateral surfaces of the fibrils for nucleation of second population crystallites.

Acknowledgements

The authors wish to express their appreciation for support of this research by the National Science Foundation through the Northwestern University Materials Research Center and through a traineeship to one of the authors, P. G. Andersen.

References

1. P. Y.-F. FUNG and S. H. CARR, *J. Macromol. Sci. (Phys.)* **B6(4)** (1972) 621.
2. A. PETERLIN, *Kolloid Z. u. Z. Polymere* **233** (1969) 857.
3. K. O'LEARY and P. H. GEIL, *J. Macromol. Sci.* **B2** (1968) 261.
4. R. E. ROBERTSON, *J. Polymer Sci. (Polym. Phys.)* **10** (1972) 2437-2452.

5. F. J. BALTÁ-CALLEJA and A. PETERLIN, *J. Macromol. Sci. (Phys.)* **B4** (1970) 519.
6. K. ISHIKAWA, K. MIYASAKA and M. MAEDA, *J. Polymer Sci.* **A2 7** (1969) 2029.
7. K. SAKAOKU and A. PETERLIN, *ibid* **A2 9** (1971) 895.
8. F. J. BALTÁ-CALLEJA, A. PETERLIN and B. CRIST, *ibid* **A2 10** (1972) 1749.
9. A. KELLER and M. J. MACHIN, *J. Macromol. Sci.* **B1** (1967) 41.
10. M. J. HILL and A. KELLER, *ibid* **B3** (1969) 153.
11. A. J. PENNINGS, J. M. A. A. VAN DER MARK and A. M. KIEL, *Kolloid Z. u. Z. Polymere* **237** (1970) 336.
12. K. KATAYAMA, T. AMANO and K. NAKAMURA, *Kolloid Z. u. Z. Polymere* **226** (1968) 125.
13. M. COMPOSTELLA, A. COEN and F. BERTINOTTI, *Angew. Chem.* **74** (1962) 618.
14. H. AWAYA and N. K. ZASSHI, *Nippon Kagaku Zasshi* **82** (1961) 1575.
15. R. J. SAMUELS, *J. Polymer Sci.* **A3** (1965) 1741.
16. V. I. SELIKHOVA, YU. A. ZUBOV, G. S. MARKOVA and V. A. KARGIN, *Vysokomol. Soyed.* **7** (1965) 216.
17. F. KHOURY, *J. Res. NBS* **70A** (Phys. and Chem.) No. 1 (1966) 29.
18. F. J. PADDEN, JUN and H. D. KEITH, *J. Appl. Phys.* **44** (1973) 1217.
19. F. L. BINSBERGEN and B. G. M. DE LANGE, *Polymer* **9** (1968) 23.
20. Z. MENCIK and D. R. FITCHMUN, *J. Polymer Sci.* **A11** (1973) 973.
21. P. FUNG, E. ORLANDO and S. H. CARR, *Polymer Eng. and Sci.* **13** (1973) 295.
22. A. J. OWEN and I. M. WARD, *J. Macromol. Sci. (Phys.)* **B7** (1973) 417.
23. N. IWATO, H. TANAKA and S. OKAJIMA, *J. Appl. Polymer Sci.* **17** (1973) 2533.
24. F. J. PADDEN, JUN and H. D. KEITH, *J. Appl. Phys.* **37** (1966) 4013.
25. J. L. KARDOS, A. W. CHRISTIANSEN and E. BAER, *J. Polymer Sci.* **A2** (1966) 777.
26. C. A. GARBER and E. S. CLARK, *J. Macromol. Sci. (Phys.)* **B4** (1970) 499.
27. A. J. MCHUGH and J. M. SCHULTZ, *Kolloid Z. u. Z. Polymere* **251** (1973) 193.
28. F. C. FRANK, A. KELLER and M. R. MACKLEY, *Polymer* **12** (1971) 467.
29. M. R. MACKLEY and A. KELLER, *Polymer* **14** (1973) 16.
30. J. A. SAUER, D. R. MORROW and G. C. RICHARDSON, *J. Appl. Phys.* **36** (1965) 3017.

Received 7 May and accepted 17 July 1974.